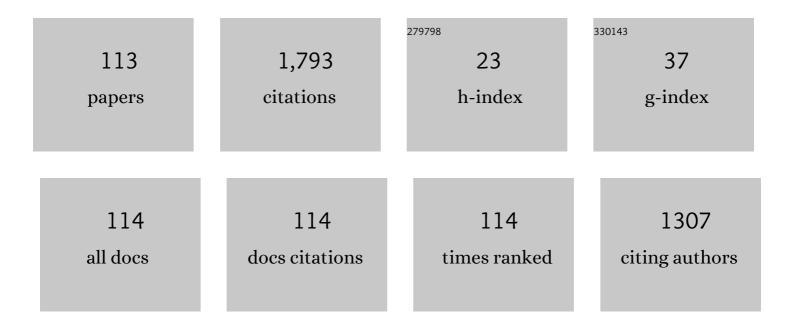
## Nikolay Surovtsev

List of Publications by Year in descending order

Source: https://exaly.com/author-pdf/3151959/publications.pdf Version: 2024-02-01



NIKOLAV SUPOVISEV

#	Article	IF	CITATIONS
1	Light-scattering spectra of fast relaxation in glasses. Physical Review B, 1998, 58, 14888-14891.	3.2	104
2	Synthesis, structural and vibrational properties of microcrystalline RbNd(MoO4)2. Journal of Crystal Growth, 2011, 318, 683-686.	1.5	91
3	Connection between quasielastic Raman scattering and free volume in polymeric glasses and supercooled liquids. Journal of Chemical Physics, 1997, 107, 1057-1065.	3.0	82
4	A comprehensive light scattering study of the glass former toluene. Journal of Chemical Physics, 2000, 113, 1143-1153.	3.0	77
5	Frequency behavior of Raman coupling coefficient in glasses. Physical Review B, 2002, 66, .	3.2	74
6	Synthesis, structural and vibrational properties of microcrystalline β-RbSm(MoO4)2. Materials Letters, 2013, 106, 26-29.	2.6	69
7	Structural and vibrational properties of microcrystalline TIM(MoO4)2 (M=Nd, Pr) molybdates. Optical Materials, 2012, 34, 812-816.	3.6	64
8	Exploration of structural, vibrational and spectroscopic properties of self-activated orthorhombic double molybdate RbEu(MoO4)2 with isolated MoO4 units. Journal of Alloys and Compounds, 2019, 785, 692-697.	5.5	64
9	Effect of nitrogen impurities on the Raman line width in diamonds. Journal of Physics Condensed Matter, 1999, 11, 4767-4774.	1.8	56
10	Temperature-Dependent Hydrocarbon Chain Disorder in Phosphatidylcholine Bilayers Studied by Raman Spectroscopy. Journal of Physical Chemistry B, 2015, 119, 15613-15622.	2.6	42
11	Glycine phases formed from frozen aqueous solutions: Revisited. Journal of Chemical Physics, 2012, 137, 065103.	3.0	37
12	Low-Temperature Dynamical and Structural Properties of Saturated and Monounsaturated Phospholipid Bilayers Revealed by Raman and Spin-Label EPR Spectroscopy. Journal of Physical Chemistry B, 2012, 116, 8139-8144.	2.6	32
13	Combined photon-echo, luminescence and Raman spectroscopies of layered ensembles of colloidal quantum dots. Laser Physics, 2019, 29, 124009.	1.2	32
14	Raman study of low-frequency modes in three glycine polymorphs. Journal of Chemical Physics, 2011, 134, 045102.	3.0	31
15	On the glass-forming ability and short-range bond ordering of liquids. Chemical Physics Letters, 2009, 477, 57-59.	2.6	28
16	Formation of amorphous sapphire by a femtosecond laser pulse induced micro-explosion. Applied Surface Science, 2009, 255, 9745-9749.	6.1	28
17	Light scattering spectra of fast relaxation in B2O3 glass. Journal of Chemical Physics, 2000, 112, 2319-2324.	3.0	27
18	Lipid Droplet Phase Transition in Freezing Cat Embryos and Oocytes Probed by Raman Spectroscopy. Biophysical Journal, 2018, 115, 577-587.	0.5	27

#	Article	IF	CITATIONS
19	On the Low-Temperature Onset of Molecular Flexibility in Lipid Bilayers Seen by Raman Scattering. Journal of Physical Chemistry B, 2008, 112, 12361-12365.	2.6	26
20	Effect of Nitrogen Impurities on the Raman Line Width in Diamond, Revisited. Crystals, 2017, 7, 239.	2.2	26
21	Transition from Arrhenius to non-Arrhenius temperature dependence of structural relaxation time in glass-forming liquids: Continuous versus discontinuous scenario. Physical Review E, 2014, 90, 032308.	2.1	25
22	Evaluation of terahertz density of vibrational states from specific-heat data: Application to silica glass. Physical Review E, 2001, 64, 061102.	2.1	24
23	Density of states and light-vibration coupling coefficient inB2O3glasses with different thermal history. Physical Review B, 2003, 67, .	3.2	24
24	Conformational Changes of Lipids in Bilayers at the Dynamical Transition Near 200 K Seen by Raman Scattering. Journal of Physical Chemistry B, 2009, 113, 15558-15562.	2.6	23
25	Raman scattering evidence of hydrohalite formation on frozen yeast cells. Cryobiology, 2013, 66, 47-51.	0.7	23
26	Density of vibrational states and light-scattering coupling coefficient in the structural glass and glassy crystal of ethanol. Journal of Physics Condensed Matter, 2004, 16, 223-230.	1.8	21
27	Temperature dependence of the Landau-Placzek ratio in glass forming liquids. Journal of Chemical Physics, 2011, 135, 134510.	3.0	21
28	Flexibility of phospholipids with saturated and unsaturated chains studied by Raman scattering: The effect of cholesterol on dynamical and phase transitions. Journal of Chemical Physics, 2014, 140, 235103.	3.0	20
29	Brillouin spectroscopy of biorelevant fluids in relation to viscosity and solute concentration. Physical Review E, 2019, 99, 062410.	2.1	20
30	qDependence of Low-Frequency Raman Scattering in Silica Glass. Physical Review Letters, 1999, 82, 4476-4479.	7.8	18
31	Raman spectroscopy reveals the lipid phase transition in preimplantation mouse embryos during freezing. Archives of Biochemistry and Biophysics, 2017, 635, 37-43.	3.0	18
32	Low-frequency Raman spectra inLiNbO3: Within and beyond the standard paradigm of ferroelectric dynamics. Physical Review B, 2005, 72, .	3.2	17
33	Transition from single-molecule to cooperative dynamics in a simple glass former: Raman line-shape analysis. Physical Review E, 2007, 76, 021502.	2.1	17
34	Redox State of Cytochromes in Frozen Yeast Cells Probed by Resonance Raman Spectroscopy. Biophysical Journal, 2015, 109, 2227-2234.	0.5	17
35	Rayleigh-Brillouin light-scattering study of a simple glass former: Evidence of locally favored structures. Physical Review E, 2010, 82, 011503.	2.1	16
36	Temperature dependence of the Raman line width in diamond: Revisited. Journal of Raman Spectroscopy, 2015, 46, 171-176.	2.5	15

#	Article	IF	CITATIONS
37	Deuterated stearic acid uptake and accumulation in lipid droplets of cat oocytes. Archives of Biochemistry and Biophysics, 2020, 692, 108532.	3.0	15
38	Raman spectroscopy evidence of lipid separation in domestic cat oocytes during freezing. Cryobiology, 2020, 95, 177-182.	0.7	15
39	Low-frequency Raman scattering study of the ferroelectric phase transition in the DKDP crystal. Physics of the Solid State, 2008, 50, 1137-1143.	0.6	14
40	Low-Frequency Raman Scattering in a Xe Hydrate. Journal of Physical Chemistry B, 2013, 117, 10686-10690.	2.6	13
41	Normal vibrational modes of phospholipid bilayers observed by low-frequency Raman scattering. Physical Review E, 2017, 95, 032412.	2.1	13
42	Suppression of spurious background in low-frequency Raman spectroscopy. Optoelectronics, Instrumentation and Data Processing, 2017, 53, 250-254.	0.6	12
43	Membrane–Sugar Interactions Probed by Low-Frequency Raman Spectroscopy: The Monolayer Adsorption Model. Langmuir, 2020, 36, 11655-11660.	3.5	12
44	Low-frequency Raman scattering in As2S3glass former around the liquid–glass transition. Journal of Physics Condensed Matter, 2003, 15, 7651-7662.	1.8	11
45	Features of the Raman coupling coefficient of boson peak vibrations in glasses. Physica Status Solidi C: Current Topics in Solid State Physics, 2004, 1, 2867-2870.	0.8	11
46	Vibrational layer eigenmodes of binary phospholipid-cholesterol bilayers at low temperatures. Physical Review E, 2019, 99, 022417.	2.1	11
47	Normal vibrations of ternary DOPC/DPPC/cholesterol lipid bilayers by low-frequency Raman spectroscopy. RSC Advances, 2019, 9, 34451-34456.	3.6	11
48	Raman study of temperature-induced hydrocarbon chain disorder in saturated phosphatidylcholines. Chemistry and Physics of Lipids, 2020, 230, 104926.	3.2	11
49	Has the boson peak a contribution from propagating modes?. Journal of Physics Condensed Matter, 1998, 10, L113-L118.	1.8	10
50	Raman line shape analysis as a mean characterizing molecular glass-forming liquids. Journal of Non-Crystalline Solids, 2011, 357, 3058-3063.	3.1	10
51	Second harmonic generation in the paraelectric phase in powders and ceramics of BaTiO3. Physics of the Solid State, 2012, 54, 920-923.	0.6	10
52	Temperature effects in low-frequency Raman spectra of corticosteroid hormones. Optics and Spectroscopy (English Translation of Optika I Spektroskopiya), 2015, 118, 214-223.	0.6	10
53	Cryoprotectant redistribution along the frozen straw probed by Raman spectroscopy. Cryobiology, 2016, 72, 148-153.	0.7	10
54	Cu <sub>2</sub> ZnSnS <sub>4</sub> crystal growth using an SnCl <sub>2</sub> based flux. CrystEngComm, 2021, 23, 1025-1032.	2.6	10

#	Article	IF	CITATIONS
55	Relaxor-like features in pressure-treated barium titanate powder. Applied Physics Letters, 2015, 107, 102902.	3.3	9
56	Structural and vibrational properties of PVT grown BiTeCl microcrystals. Materials Research Express, 2019, 6, 045912.	1.6	9
57	Deciphering the orientation of lipid molecules by principal component analysis of Raman mapping data. Analyst, The, 2020, 145, 1466-1472.	3.5	9
58	Salient Properties of Raman Central Peak in LiNbO3and LiTaO3Crystals. Ferroelectrics, 2007, 348, 177-181.	0.6	8
59	Temperature of nanometer-scale structure appearance in glasses. Glass Physics and Chemistry, 2013, 39, 124-129.	0.7	8
60	Exploration of the Structural and Vibrational Properties of the Ternary Molybdate Tl <sub>5</sub> BiHf(MoO <sub>4</sub> ) <sub>6</sub> with Isolated MoO <sub>4</sub> Units and Tl <sup>+</sup> Conductivity. Inorganic Chemistry, 2020, 59, 12681-12689.	4.0	8
61	Raman spectroscopy and DSC assay of the phase coexistence in binary DMPC/cholesterol multilamellar vesicles. Biochimica Et Biophysica Acta - Biomembranes, 2021, 1863, 183514.	2.6	8
62	Suppression of fast relaxation and the Raman coupling coefficient in densified silica. Journal of Physics Condensed Matter, 2004, 16, 3035-3040.	1.8	7
63	Fast relaxation intensity versus silica glass density: existence of sharp peculiarity. Journal of Physics Condensed Matter, 2006, 18, 4763-4771.	1.8	7
64	Central Peak in Raman Spectra of Ferroelectric KDP and DKDP Crystals. Ferroelectrics, 2009, 379, 43-47.	0.6	7
65	Uniaxial mechanical stresses and their influence on the parameters of the ferroelectric phase transition in pressure-treated barium titanate. Ferroelectrics, 2017, 508, 161-166.	0.6	7
66	Specific features in the behavior of the central peak in Raman spectra of lithium tantalate. Physics of the Solid State, 2006, 48, 2317-2321.	0.6	6
67	Dielectric susceptibility of a deuterated KDP crystal from experiment on Raman scattering and in the cluster approximation. Physics of the Solid State, 2011, 53, 1371-1377.	0.6	6
68	Local residual stresses in pressure-treated barium titanate powders probed by second harmonic generation. Ferroelectrics, 2016, 501, 9-14.	0.6	6
69	Raman spectroscopy for quantification of water-to-lipid ratio in phospholipid suspensions. Vibrational Spectroscopy, 2018, 97, 102-105.	2.2	6
70	Effect of low temperatures on cytochrome photoresponse in mouse embryos. Archives of Biochemistry and Biophysics, 2019, 669, 32-38.	3.0	6
71	Raman spectra of deuterated hydrocarbons for labeling applications. Journal of Raman Spectroscopy, 2022, 53, 297-309.	2.5	6
72	Temperature Dependence of Hyperfine Interaction for 15N Nitroxide in a Glassy Matrix at 10–210ÂK. Applied Magnetic Resonance, 2011, 41, 411-429.	1.2	5

#	Article	IF	CITATIONS
73	Photobleaching of the resonance Raman lines of cytochromes in living yeast cells. Journal of Photochemistry and Photobiology B: Biology, 2014, 141, 269-274.	3.8	5
74	Origin of the anomaly in the behavior of the viscosity of water near 0°C. JETP Letters, 2015, 102, 732-736.	1.4	5
75	Second harmonic generation study of local polar inhomogeneities in Pb3(MgNb2)O9. Physics of the Solid State, 2015, 57, 472-475.	0.6	5
76	Stretch Vibrations of CH2 as a Measure of Conformational and Lateral Orders in Fatty Acid and Phospholipid Layers. Optoelectronics, Instrumentation and Data Processing, 2018, 54, 538-545.	0.6	5
77	Brillouin study of elastic properties of nanometric phospholipid layers in aqueous suspensions of vesicles. Ferroelectrics, 2019, 541, 10-16.	0.6	5
78	Residual mechanical stresses in pressure treated BaTiO3 powder. Ceramics International, 2019, 45, 12455-12460.	4.8	5
79	Effect of the Hydrocarbon Chain Disorder in Phosphatidylcholine Bilayers on Gigahertz Sound Velocity. Journal of Physical Chemistry B, 2020, 124, 9079-9085.	2.6	5
80	Raman Spectroscopic Study of Phase Coexistence in Binary Phospholipid Bilayers. Applied Spectroscopy, 2021, 75, 87-93.	2.2	5
81	Lipid phase transitions in cat oocytes supplemented with deuterated fatty acids. Biophysical Journal, 2021, 120, 5619-5630.	0.5	5
82	Low-frequency inelastic light scattering in a ZBLAN (ZrF4-BaF2-LaF3-AlF3-NaF) glass. Journal of Chemical Physics, 2014, 140, 184508.	3.0	4
83	Glass crystallization in the MnNbOF5-BaF2-BiF3 system as probed by Raman spectroscopy. Russian Journal of Inorganic Chemistry, 2014, 59, 831-837.	1.3	4
84	Local residual stresses in pressure-treated barium titanate powders probed by inelastic light scattering. Ferroelectrics, 2016, 496, 225-230.	0.6	4
85	Temperature dependence of the Landau-Placzek ratio in liquid water. Physical Review E, 2017, 96, 042608.	2.1	4
86	Ionic liquid glasses: properties and applications. Russian Chemical Reviews, 2022, 91, .	6.5	4
87	Raman scattering in protonated and deuterated 1,2-dipalmitoyl-sn-glycero-3-phosphatidylcholine (DPPC): Indicators of conformational and lateral orders. Spectrochimica Acta - Part A: Molecular and Biomolecular Spectroscopy, 2022, 267, 120583.	3.9	4
88	Dynamic response on a nanometer scale of binary phospholipid-cholesterol vesicles: Low-frequency Raman scattering insight. Physical Review E, 2021, 104, 054406.	2.1	4
89	Specific features of the central peak in the Raman spectra of a lithium niobate crystal. Physics of the Solid State, 2006, 48, 1094-1098.	0.6	3
90	Investigation of the fast relaxation in glass-forming selenium by low-frequency Raman spectroscopy. Glass Physics and Chemistry, 2008, 34, 30-36.	0.7	3

#	Article	IF	CITATIONS
91	Central peak in the strontium titanate crystal near the tetragonal-to-cubic phase transition. Physics of the Solid State, 2012, 54, 924-926.	0.6	3
92	Inelastic light scattering study of hydrogen-bonded glass formers: Glycerol and ethanol. Journal of Non-Crystalline Solids, 2017, 471, 429-434.	3.1	3
93	Effect of glycerol on photobleaching of cytochrome Raman lines in frozen yeast cells. European Biophysics Journal, 2018, 47, 655-662.	2.2	3
94	Vibrational eigenmodes of phospholipid layers in lowâ€wavenumber Raman spectrum of multilamellar vesicles. Journal of Raman Spectroscopy, 2019, 50, 1691-1699.	2.5	3
95	Optical investigations of fluctuation of order parameter in THz range in SrxBa1-xNb2O6 crystals with different chemical compositions. Ferroelectrics, 2020, 560, 102-109.	0.6	3
96	Temperature dependence of elastic properties of the phospholipid vesicles in aqueous suspension probed by Brillouin spectroscopy. Journal of Physics Condensed Matter, 2021, 33, 495102.	1.8	3
97	A monoclinic semiorganic molecular crystal GUHP for terahertz photonics and optoelectronics. Scientific Reports, 2021, 11, 23433.	3.3	3
98	Coexistence of lipid phases in multilayer phospholipid films probed by Raman mapping. Analyst, The, 2022, 147, 3748-3755.	3.5	3
99	On the universal regularities of the lattice dynamics in ferroelectrics. Physics of the Solid State, 2009, 51, 1390-1393.	0.6	2
100	Lowâ€wavenumber Raman scattering of phospholipid bilayers in fluid, ripple, and gel phases. Journal of Raman Spectroscopy, 2020, 51, 952-958.	2.5	2
101	On the Mutual Relationships between Molecular Probe Mobility and Free Volume and Polymer Dynamics in Organic Glass Formers: cis-1,4-poly(isoprene). Polymers, 2021, 13, 294.	4.5	2
102	Brillouin Spectroscopy of Binary Phospholipid–Cholesterol Bilayers. Applied Spectroscopy, 2022, 76, 1206-1215.	2.2	2
103	Order Parameter Dynamics and Hydrogen Bond Potential in DKDP. Ferroelectrics, 2012, 440, 113-118.	0.6	1
104	Dynamics of the order parameter and the potential of the hydrogen bond in a ferroelectric DKDP crystal. Journal of Experimental and Theoretical Physics, 2013, 116, 280-285.	0.9	1
105	Structural Properties of Glass-Forming Ethanol and Glycerol From O–H Vibrational Spectra. Journal of Structural Chemistry, 2018, 59, 321-327.	1.0	1
106	Frequencies of Stretching and Bending OH (OD) Vibrations in KDP (DKDP) Crystals, According to the Temperature Dependence of Their Raman Spectrum. Bulletin of the Russian Academy of Sciences: Physics, 2018, 82, 294-298.	0.6	1
107	Second-order-derivative analysis of structural relaxation time in the elastic model of glass-forming liquids. Physical Review E, 2020, 101, 052610.	2.1	1
108	Determination of the Orientation of Phospholipid Molecules in Planar Structures from Raman Spectra. Optoelectronics, Instrumentation and Data Processing, 2019, 55, 495-500.	0.6	1

#	Article	IF	CITATIONS
109	Conformational state diagram of DOPC/DPPCd62/cholesterol mixtures. Biochimica Et Biophysica Acta - Biomembranes, 2022, 1864, 183869.	2.6	1
110	Stimulated Raman scattering of light in optical silica fiber under subnanosecond pumping. Optoelectronics, Instrumentation and Data Processing, 2013, 49, 416-422.	0.6	0
111	Nanometer structure as a key to various phenomena in ferroelectrics. Ferroelectrics, 2021, 575, 37-42.	0.6	Ο
112	Possibilities of Brillouin spectroscopy in the study of xenogeneic collagen-containing materials. , 2022, , .		0
113	Strontium barium niobate crystals with various chemical compositions probed by Raman and Brillouin scattering. Ferroelectrics, 2022, 592, 108-115.	0.6	0